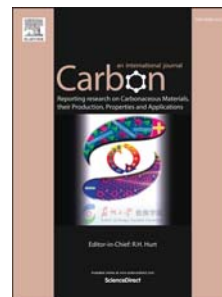


# Accepted Manuscript

Two-dimensional oligoglycine tectomer adhesives for graphene oxide fiber functionalization

R. Garriga, I. Jurewicz, S. Seyedin, M. Tripathi, J.R. Pearson, V.L. Cebolla, A.B. Dalton, J.M. Razal, E. Muñoz



PII: S0008-6223(19)30211-8

DOI: <https://doi.org/10.1016/j.carbon.2019.02.080>

Reference: CARBON 13995

To appear in: *Carbon*

Received Date: 23 November 2018

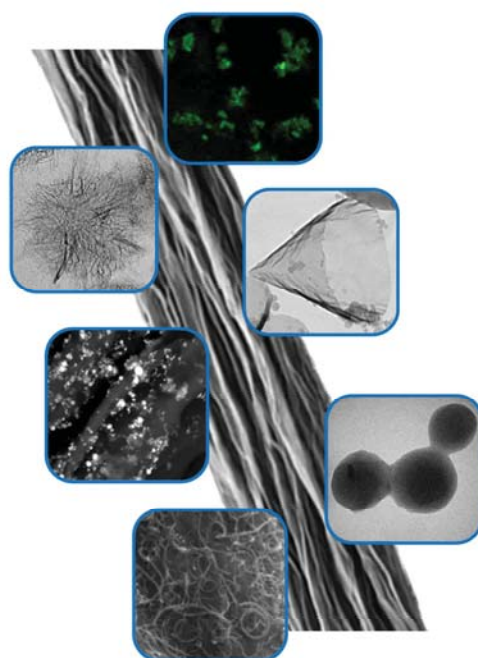
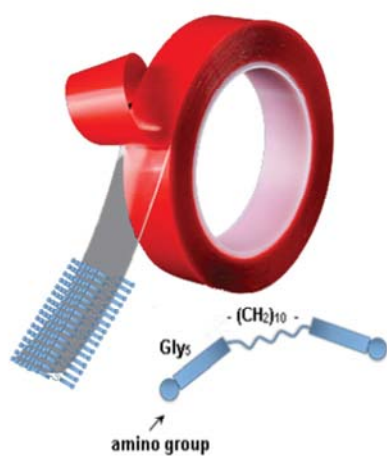
Revised Date: 10 February 2019

Accepted Date: 25 February 2019

Please cite this article as: R. Garriga, I. Jurewicz, S. Seyedin, M. Tripathi, J.R. Pearson, V.L. Cebolla, A.B. Dalton, J.M. Razal, E. Muñoz, Two-dimensional oligoglycine tectomer adhesives for graphene oxide fiber functionalization, *Carbon* (2019), doi: <https://doi.org/10.1016/j.carbon.2019.02.080>.

This is a PDF file of an unedited manuscript that has been accepted for publication. As a service to our customers we are providing this early version of the manuscript. The manuscript will undergo copyediting, typesetting, and review of the resulting proof before it is published in its final form. Please note that during the production process errors may be discovered which could affect the content, and all legal disclaimers that apply to the journal pertain.

**Tectomer**  
double-sided sticky tape  
for GO fiber decoration



# Two-dimensional oligoglycine tectomer adhesives for graphene oxide fiber functionalization

R. Garriga <sup>a,\*</sup>, I. Jurewicz <sup>b</sup>, S. Seyedin <sup>c</sup>, M. Tripathi <sup>d</sup>, J.R. Pearson <sup>e</sup>, V.L. Cebolla <sup>f</sup>, A.B.  
Dalton <sup>d</sup>, J.M. Razal <sup>e</sup>, E. Muñoz <sup>f,\*</sup>

<sup>a</sup> *Departamento de Química Física, Universidad de Zaragoza, 50009 Zaragoza, Spain*

<sup>b</sup> *Department of Physics, Faculty of Engineering & Physical Sciences, University of Surrey,  
Guildford GU2 7XH, United Kingdom*

<sup>c</sup> *Deakin University, Institute for Frontier Materials, Geelong 3220 Victoria, Australia*

<sup>d</sup> *Department of Physics, University of Sussex, Brighton, BN1 9RH, United Kingdom*

<sup>e</sup> *Andalusian Centre for Nanomedicine and Biotechnology (BIONAND), Parque Tecnológico de  
Andalucía, 29590 Campanillas, Málaga, Spain*

<sup>f</sup> *Instituto de Carboquímica ICB-CSIC, Miguel Luesma Castán 4, 50018 Zaragoza, Spain*

---

\* Corresponding author.

E-mail: [rosa@unizar.es](mailto:rosa@unizar.es) (R. Garriga)

E-mail: [edgar@icb.csic.es](mailto:edgar@icb.csic.es) (E. Muñoz)

## ABSTRACT

Amino-terminated oligoglycine two-dimensional (2D) peptide self-assemblies (known as tectomers) have a versatile surface chemistry that allows them to interact with a variety of nanomaterials and to act as supramolecular adhesives for surface functionalization. Here, we have exploited the strong hydrogen-bond based interaction between tectomers and graphene oxide (GO) to functionalize GO fiber surfaces with different carbon nanomaterials (carbon nanotubes, carbon nanohorns, carbon nanocones, and highly fluorescent nanodiamonds), metal (gold, platinum, iron) nanoparticles, acrylate-based polymer nanoparticles, fluorophores and drugs. The resulting ultrathin coatings exhibit remarkable water resistant properties. This tectomer-mediated fiber decoration strategy allows coating functionalities to be tailored by choosing the appropriate nanomaterials or other molecules. We show that this strategy can be extended to other fibers and fabrics, such as polyurethane/PEDOT:PSS, poly(methyl methacrylate) and polyester, making it very attractive for a variety of technological and smart textile applications.

## 1. Introduction

The versatile surface chemistry of bioinspired polymers and biomolecules such as polydopamine [1,2], chitosan [3-6], or Arg-Gly-Asp (RGD) peptides [7,8], allows them to exhibit adhesive and binder properties suitable for the fabrication of functional coatings for a variety of biomedical (drug delivery, tissue engineering, cell adhesion, theranostics, surgical adhesives,...) and technological applications (such as in energy storage devices, in membrane separation technologies, in catalysis, or as reinforcement binders, to name a few) [9,10].

Functionalization of a range of substrates and surfaces can be achieved by the covalent functionalization of the coatings, or through the attachment or immobilization of nanoparticles, biomolecules, or cells using these adhesives.

Oligoglycines are examples of synthetic peptides with exceptional self-assembly capabilities. Amino-terminated oligoglycines non-covalently self-assemble into biocompatible, rigid two-dimensional (2D) nanostructures called tectomers [11,12], formed either in solution or in surface-promoted processes, stabilized by a cooperative hydrogen bond system. Tectomers have been successfully utilized to coat negatively-charged surfaces, such as mica [12,13] and bacteria membranes [14], and to viruses through oligoglycine glycosylation [15,16], and polymer fibers by covalent functionalization [17]. In recent years, our research group has explored the unique assembly features and versatile surface chemistry of tectomers, demonstrating tectomers as efficient pH-responsive 2D nanocarriers of anticancer drugs and fluorophores, making them extremely attractive for biosensing and therapeutic applications [18]. We also reported on the functionalization of transparent silver nanowire (AgNW) electrodes with tectomer nanosheets [19], where the tectomer coating markedly increases the overall electrode electrical conductivity through mechanical squeezing of wire-wire junctions in the AgNW network. The strong AgNW/tectomer interaction results from the donation of electron density from tectomer N atoms toward the wires. Moreover, these tectomer coatings provide enhanced electrode hydrophobicity and protect AgNW against oxidation and degradation when exposed to atmospheric conditions [19]. Also, we showed that 2D oligoglycine tectomers strongly interact with graphene oxide (GO) through hydrogen bond formation between the tectomer amino terminal groups and the epoxy- and hydroxyl groups of the GO basal plane, thus the interaction between both 2D materials is maximized in GO/tectomer hybrids [20]. On the other hand, the strong electrostatic

interactions between tectomer amino groups and the carboxylic acid groups of carboxylated multi-walled carbon nanotubes (MWCNT-COOH) lead to the formation of extensive, surface adaptive, ultrathin tectomer coatings on MWCNT-COOH and stable MWCNT-COOH/tectomer inks. Moreover, wettability studies conducted on tectomer-coated glass substrates showed that the deposited tectomer films provide enhanced hydrophobicity [20].

GO fibers are macroscopic GO layered assemblies that combine high mechanical strength and flexibility that allow them to be knitted into fabrics and complex 3D architectures [21-25]. Their unique, highly porous structure together with the electrical conductivity when reduced results in high electrochemical double layer capacitance, meaning that they can act as electrodes in energy storage devices integrated into flexible electronics, wearables and smart garments [26,27]. We exploited the strong affinity of tectomers for both MWCNT-COOH and GO, to coat wet-spun GO fibers with MWCNT-COOH using tectomers as an adhesive. We additionally showed that these tectomer-functionalized GO fibers can be used as 2D and ultimately 3D scaffolds, therefore providing interesting opportunities in tissue engineering, such as *in vitro* human cancer cell culture models [20].

Here, we present a simple method for GO fiber functionalization with a variety of nanomaterials and molecules, such as MWCNT-COOH, single-walled carbon nanohorns (SWCNH), carbon nanocones (CNC), highly fluorescent nanodiamonds (FND), metal nanoparticles (FeNP, AuNP, PtNP), polymeric nanoparticles, and fluorophores and drugs, that exploits the adhesive properties of tectomers. Our method allows fiber physicochemical properties to be easily fine-tuned, making it attractive for a range of technological and biomedical applications. We show that this tectomer-based surface decoration strategy can be extended to other kinds of fibers, including polyurethane/poly3,4-

ethylenedioxythiophene:poly(styrenesulfonate) (PU/PEDOT:PSS) composite fibers [28], poly(methyl methacrylate) (PMMA) fiber, and polyester (PES) fibers and fabrics. Our results demonstrate new uses for tectomers as versatile platforms for achieving robust coatings that are critical for a range of technological- and smart textile applications

## 2. Materials and methods

### 2.1. Materials

Biantennary oligoglycine peptide  $C_8H_{16}(-CH_2-NH-Gly_5)_2 \cdot 2HCl$ , purity > 95 %, was supplied by PlasmaChem GmbH and used as received. Oligoglycine solutions in ultrapure water (Siemens LaboStar DI/UV 2 system, resistivity: 18.2 M $\Omega$  cm at 25 °C) were prepared by bath sonication (100 W Branson 2510 bath sonicator) for 3 min.

GO fibers were decorated with the following commercial carbon nanomaterials: MWCNT-COOH (PlasmaChem GmbH, up to 20 nm in diameter, 3-15 walls, 1-10  $\mu$ m in length, purity >95%, and 18.0 wt. % oxygen, 70.5 wt. % carbon), CNC (n-TEC, produced by hydrocarbon pyrolysis [29]), FND particles (Adámas Nanotechnologies, high brightness 3 ppm of NV-minus centers, 100 nm average size, 1 mg·mL<sup>-1</sup> in DI water suspension), and SWCNH (Carbonium S.r.l., 2-5 nm in diameter, 30-50 nm in length, forming dahlia-like aggregates ~100 nm in diameter, purity >99%, and ~0.5 at. % Oxygen, produced without any catalyst, by rapid condensation of small carbon clusters (C<sub>2</sub> and C<sub>3</sub>) obtained by direct vaporization of graphite [30]). Additionally, GO fibers were decorated with hydrophilic NP: PtNP (PlasmaChem GmbH, 4 nm, coated with polyvinylpyrrolidone (PVP)), FeNP (PlasmaChem GmbH, ferromagnetic Fe-state, 30 to 60 nm, with hydrophilic carbon shell containing hydroxy and carboxy-groups on the

surface), AuNP (13 nm, synthesized by reduction of tetrachloroauric acid ( $\text{H}[\text{AuCl}_4]$ , Sigma-Aldrich, 99.999 %) with sodium citrate (Sigma-Aldrich, 99.0 %) [31], and acrylate-based polymer NP (PolymP-Active, provided by NanoMyP<sup>®</sup>). Coralyne chloride (2,3,10,11-tetramethoxy-8-methylisoquino[3,2-*a*]isoquinolinium chloride, 38989-38-7 CAS) was purchased from Sigma-Aldrich, and was purified by recrystallization with methanol (spectroscopic grade). Coralyne was always kept in darkness and solutions were prepared prior for use.

GO fibers were wet-spun by coagulation of  $5 \text{ mg}\cdot\text{mL}^{-1}$  liquid crystalline GO dispersions in calcium chloride bath, rinsed with ethanol, and then dried in air under tension [24]. According to X-ray photoelectron spectroscopy (XPS) analysis, the C:O atomic ratio for the GO material used was 2.01. GO fibers were reduced both thermally or chemically: thermal reduction was performed under vacuum at  $240 \text{ }^\circ\text{C}$  during 12 h, while chemical reduction was achieved by exposure of GO fibers to hydrazine vapors at  $80 \text{ }^\circ\text{C}$  for 3 h [22]. Fiber spinning of PU/PEDOT:PSS fibers, at 13 wt. % (PEDOT:PSS), was carried out by a wet-spinning method reported elsewhere [28]. Commercial PMMA optical fibers were purchased from Elenco Electronics Inc. and PES fabric was supplied by Kalenji. Two- and four-probe electrical resistance measurements were performed using a Keithley 2000 multimeter.

## 2.2. Fiber coating procedures

Typical tectomer coating experiments were performed by impregnation of  $\sim 2 \text{ cm}$  long GO fibers in 3 mL of  $1.0 \text{ mg}\cdot\text{mL}^{-1}$  oligoglycine solution for 18 h. The tectomer coated fibers were then washed twice by immersion in 3 mL of ultrapure water, each time for 90 min, to remove the excess of tectomer non-specifically attached to the fiber, and then let to dry in air at room temperature.

Two different GO fiber decoration strategies were used: GO fibers were first coated with tectomers as mentioned above, and then in a second step impregnated in 3 mL of aqueous dispersions of the targeted nanomaterials for 3 h. The coated fibers were washed twice by immersion in 3 mL of ultrapure water, each time for 90 min, and then let to dry in air at room temperature. Hence, tectomers act as supramolecular adhesives, able to interact on one side with the GO fiber surface and on the opposite side with the nanomaterials in solution. Alternatively, GO fibers were coated with the tectomer hybrids of the different nanomaterials in a single step by impregnation for 18 h in aqueous dispersions of the tectomer/nanomaterial hybrids. This one-step approach was performed for GO fiber decoration with highly hydrophobic nanomaterials, such as SWCNH and CNC, that poorly disperse in water, so that tectomers combine their adhesive properties and their ability to assist in the dispersion of these nanomaterials in water. The one-step procedure was also followed for FeNP, which has a high tendency to aggregate in aqueous solutions in the absence of tectomers. Each coating step was followed by washing the fibers twice in 3 mL of ultrapure water, each time for 90 min, to remove non-specifically bound materials and to assess the stability of the coatings. These fiber coating procedures were also applied to rGO and PU/PEDOT:PSS fibers, as well as to commercial PMMA fibers and PES fibers.

### *2.3. Electron microscopy characterization*

Transmission electron microscopes (TEM, Tecnai T20 and Tecnai F30, FEI, operating at 200 and 300 KV, respectively) were used to characterize tectomer structures and their interaction with different nanomaterials. During sample preparation, a drop of aqueous dispersions of the materials used was placed onto carbon coated copper grids, the sample excess was wicked away by means of a kinwipe and allowed to dry under ambient conditions. Prior to TEM imaging, the

samples on the grids were placed in a O<sub>2</sub>-Ar (20% O<sub>2</sub>) plasma cleaner (Fischione, Model 1020) for 5-10 s to remove organic (hydrocarbon) contamination.

Scanning electron microscopy (SEM) characterization was performed with an Inspect F50 field emission SEM microscope (FEI). Non-conductive PMMA fibers and PES fabrics were coated with a 14 nm thick Pd layer by sputtering. Combining backscattered electron (BSE) imaging and energy-dispersive X-ray spectroscopy (EDS), we obtained a qualitative estimation of the amount of metal nanoparticles attached on the tectomer-treated fibers.

#### *2.4. Conductive atomic force microscopy characterization*

rGO fibers placed over Indium Tin Oxide (ITO) substrates were glued by silver paint at the edges of the fiber to restrict any rotation/displacement during conductive atomic force microscopy (AFM) measurements. The edges of the ITO substrate were coated with silver paint to establish good electrical connection with the AFM (Bruker ScanAsist) stage. Conductive probes (silicon nitride coated with Pt/Ir, model: PF-TUNA,  $K_n = 0.6 \text{ N m}^{-1}$  and  $0.3 \text{ N m}^{-1}$  from Bruker) were used in the measurement. TUNA measurement, a term coined by the equipment manufacturer (Bruker), is a hybrid of conductive AFM-STM measurement associated with tunneling atomic force microscopy. AFM measurements were carried out in the Peak-force TUNA mode at a fixed sample bias of 500 mV and the distribution of the conductive regions were hence recorded. TUNA allows a tunnelling current to be obtained from a nanosharp tip attached to a cantilever while simultaneously moving the tip across the sample surface to measure topographical data. In our conductive measurement, TUNA was combined with a sensitive feedback control mechanism, termed PeakForce by the manufacturers (Bruker) that regulates interactions between the conductive AFM tip and the sample across which emitted

electrons must travel. PeakForce is a non-harmonic feedback system in which force curves are taken regularly along a scan-line allowing the feedback parameter (the interaction force between tip and sample surface) to be kept at a set-point (1.2 nN). Comprehensive details of the PF-TUNA measurement system are available elsewhere [32].

### *2.5. Confocal fluorescence and brightfield microscopy*

Oligoglycine solutions containing fluorophores (coralyne and FND) were analyzed by optical microscopy. Confocal fluorescence and brightfield images were obtained using a Leica SP5 laser scanning confocal microscope equipped with spectral HyD detectors. Acquisition was performed using a 63X 1.4 NA HCX PL APO oil immersion objective allowing fluorescence to be captured as discrete ~600 nm optical sections. Adjustments to the spectral emission detection window allowed loaded fluorophore self-assemblies to be distinguished from background fluorescence in solution. The following excitation and emission conditions were used: Coralyne = Ex 405 nm/Em 523-571 nm, FND = Ex 514 nm /Em 620-795 nm. We confirmed that peptide samples in absence of fluorophore did not emit detectable levels of fluorescence under these conditions. Images of GO fibers coated with the different fluorophores were obtained using a lower magnification 10x 0.40 NA HCL PL APO CS dry objective. Images are shown as either single sections or maximum projections of multiple optical sections.

### *2.6. X-ray photoelectron spectroscopy*

X-ray photoelectron spectroscopy (XPS) was performed on aqueous solutions dried on Al foil using an ESCA Plus Omicron spectrometer provided with an Al anode (1486.7 eV) working at 225 W (15 mA, 15 kV). When required, binding energy (BE) positions were corrected by

setting the aromatic C 1s component at a BE of 284.5 eV or  $sp^3$  carbon at 284.8 eV. CASA software was used for the peak deconvolution and Shirley type baseline correction was applied.

### 3. Results and discussion

Wet-spun GO fibers were  $\sim 60$  micrometers in diameter (Fig. 1(a, b)). SEM image of the cross-section of GO fiber is shown Fig. 1(c, d), revealing GO sheet planes that are oriented along the fiber axis.

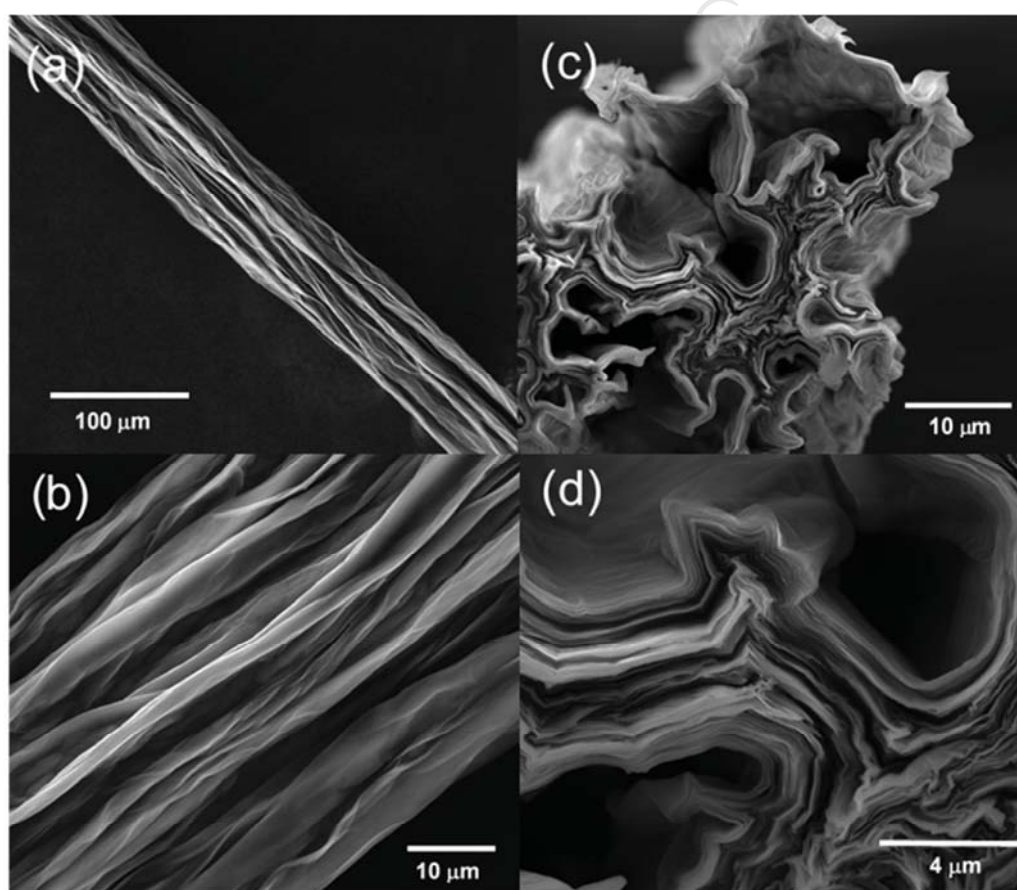


**Fig. 1.** SEM images of wet spun GO fibers,  $\sim 60$   $\mu\text{m}$  average diameter (a), GO fiber surface morphology (b), and cross-section (c, d).



**Fig. 2.** Molecular structures of biantennary oligoglycine, and scheme showing association of 2D self-assemblies (tectomers), stabilized by extensive networks of hydrogen bonds between the antennae (a). SEM images of tectomer coatings on a GO fiber (b).

GO fiber reduction leads to increased fiber electrical conductivity, lower GO sheet  $d$ -spacing and decreased porosity [27]. As mentioned above, GO fibers were reduced both thermally and chemically, and conductivity values of these fibers were respectively  $\sigma = 5 \text{ S}\cdot\text{cm}^{-1}$  and  $\sigma = 100 \text{ S}\cdot\text{cm}^{-1}$ , indicating that the chemical reduction is more effective [33]. Tectomer coatings obtained for rGO fibers (Fig. S1) were similar to those of GO fibers (Fig. 2(b)), in spite of the lower amount of oxygen functional groups on the rGO fiber surface. Additionally, electron density donation from amino groups in tectomers to the  $\pi$  system of rGO comes into play. We verified that rGO fiber electrical conductivity was unaffected by tectomer coating, even when immersed in tectomer solutions.

### *3.1. Decoration of GO fibers with carbon nanomaterials*

Strong electrostatic interactions occur between tectomers and MWCNT-COOH, leading to the formation of soluble aqueous MWCNT-COOH/tectomer inks, where tectomers extensively coat MWCNT-COOH [20]. Electrostatic interaction between the positive charges of protonated tectomer amino groups and the negative charges of carboxylic groups leads to a curvature in the tectomer assembly resulting in adaptive coatings around the carbon nanotubes (CNT). We also observed that GO fibers easily disassemble and fall apart upon direct immersion in aqueous MWCNT-COOH dispersions, due to the well-known affinity between CNT and GO

[34]. However, in the presence of tectomers, GO fibers can be coated with MWCNT-COOH, as tectomers act as protective adhesive layer [20].

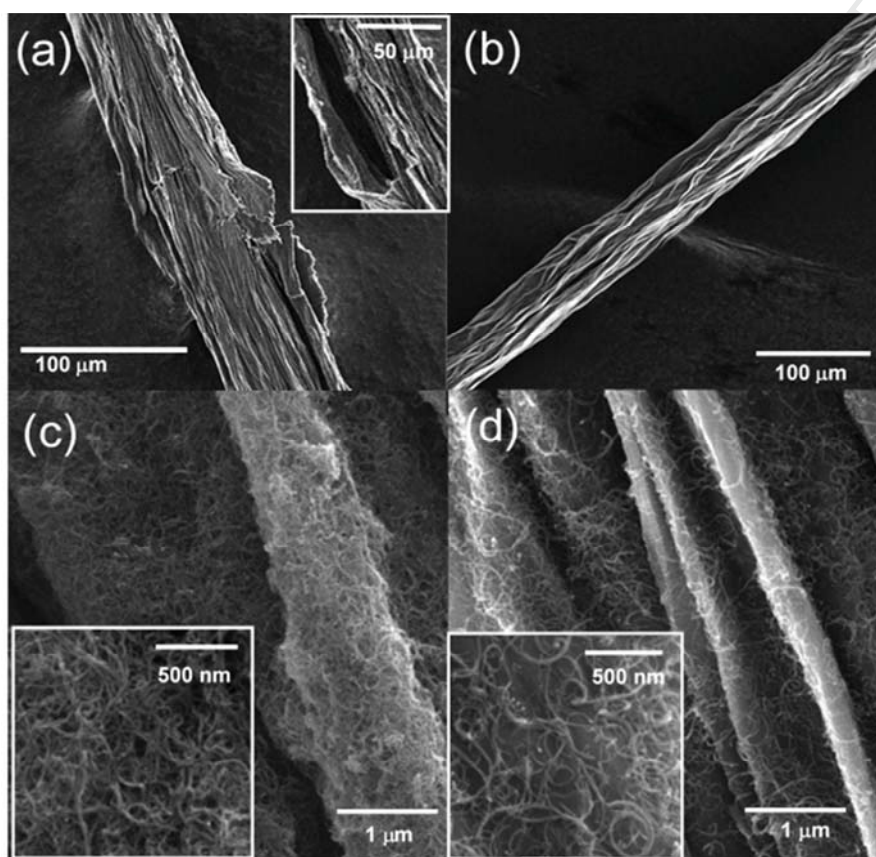


**Fig. 3.** SEM micrographs of a chemically reduced rGO fiber coated with MWCNT-COOH by direct immersion in a  $1 \text{ mg}\cdot\text{mL}^{-1}$  MWCNT-COOH dispersion (a, c), or by a two-step procedure, first coated with tectomers by immersion in  $1 \text{ mg}\cdot\text{mL}^{-1}$  oligoglycine solution, and then impregnated in a  $1 \text{ mg}\cdot\text{mL}^{-1}$  MWCNT-COOH dispersion (b, d). Insets in (c, d) show a higher density of MWCNT-COOH on the fiber surface upon direct immersion in the MWCNT-COOH dispersion, however this impregnation process leads to partial fiber damage (a).

On the other hand, we verified that direct immersion of rGO fibers in aqueous MWCNT-COOH dispersions in absence of tectomers still leads to significant damage on the fibers, though they are not completely destroyed (Fig. 3 (a)). As mentioned above, the lower content in oxygen functional groups in rGO leads to a drastic decrease in *d*-spacings of GO sheets [27], resulting in a higher structural stability than GO fibers. Fig. 3(d) shows a somewhat lower density of MWCNT-COOH on the fiber surface than Fig. 3(c), however the fibers are not damaged due to tectomer protection (Fig. 3(b)). The facile, soft chemistry procedure for CNT functionalization of GO fibers described here can be considered as an alternative to other strategies for CNT fiber decoration [20]. Conductive AFM measurements were performed to gain insights into the electrical properties of the fiber coatings. The maximum current intensity values for the MWCNT-COOH/TECTOMER coated rGO fiber (Fig. 4(b)) and for the MWCNT-COOH coated rGO fiber (Fig. 4(c)) were similar, showing a 2-fold increase versus the value measured for the uncoated rGO fiber (Fig. 4(a)).

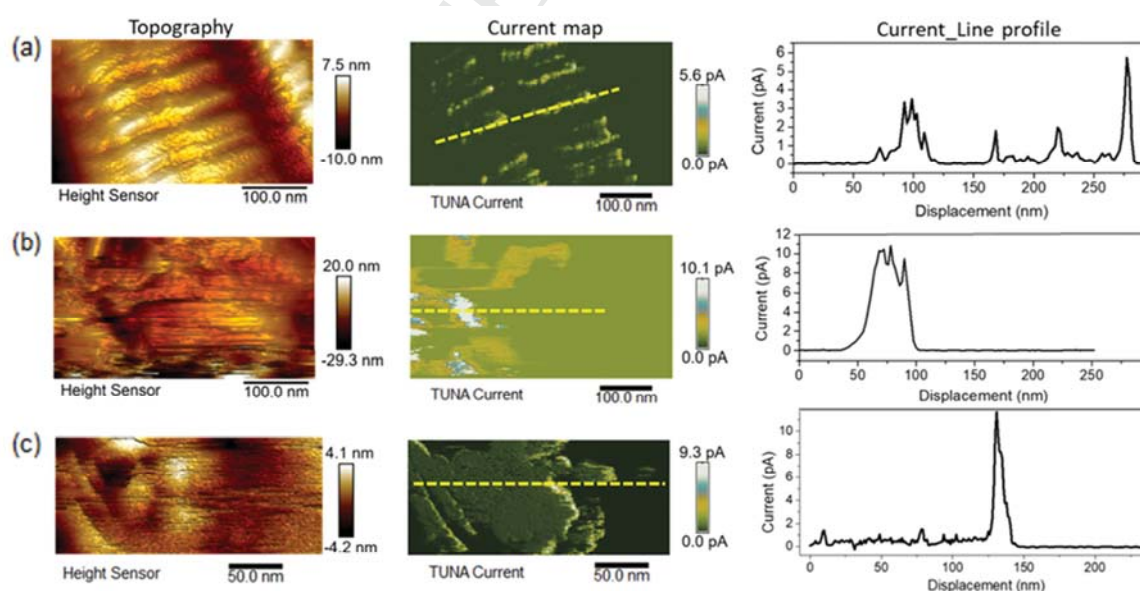


**Fig. 4.** Topography and conducting AFM (PeakForce tapping) images: rGO fiber (a), rGO fiber coated with MWCNT-COOH/tectomer (b), and rGO fiber coated with MWCNT-COOH (c). All topography and peakforce TUNA current images were carried out at fixed DC bias voltage (500 mV) applied to the sample. The brighter colors correspond to higher height in topography and higher conductive regions in the current map, confirmed by their corresponding line profile. MWCNT-COOH/tectomer and MWCNT-COOH coated rGO fibers provide higher current values (pA) when compared to that of the uncoated rGO fiber (2-fold increase).

The nitrogen-vacancy (N-V) defects of fluorescent nanodiamonds (FND) are responsible for their red/near-infrared fluorescence properties. These non-photo-bleaching nanoparticles are attractive for *in vitro* and *in vivo* fluorescence imaging [35]. In this work we used high brightness, 100 nm average size FND. These nanoparticles have abundant oxygen functional groups on the surface and attach well to tectomers, as confirmed by TEM (Fig. 5(a, b)), bright-field (Fig. 5(c)), SEM (Fig. 5(d)) and confocal fluorescence images (Fig. 5(e)). The concentration of FND in tectomers allowed measurement of their intense fluorescence emission spectrum, showing a maximum at 680 nm (Fig. S2). As in the case of MWCNT-COOH, direct immersion of GO fibers in a FND dispersion leads to the destruction of the fiber (Fig. S3), due to the strong interaction between FND and GO. Again, tectomers can act as a protective adhesive, allowing FND decoration of GO fibers while maintaining their structure. The fluorescence properties of FND decorated GO fibers are shown in Fig. 5(f).

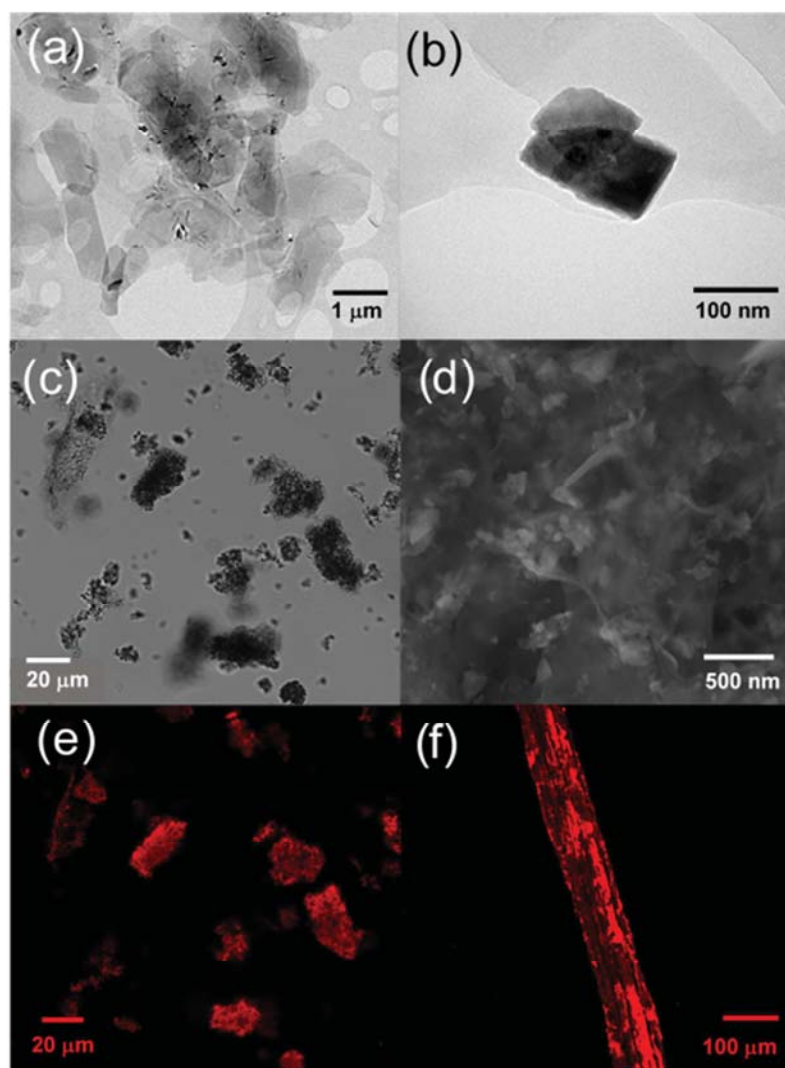


**Fig. 5.** TEM (a, b), bright-field microscopy (c), SEM (d), and confocal fluorescence microscopy (e) images corresponding to  $0.25 \text{ mg} \cdot \text{mL}^{-1}$  FND/ $1 \text{ mg mL}^{-1}$  oligoglycine dispersions in water. These images show FND attached to tectomer platelets, suggesting strong FND/tectomer interaction. Confocal fluorescence image of a GO fiber, first coated with tectomers, and then impregnated in a  $0.25 \text{ mg mL}^{-1}$  FND dispersion (f), showing that FND provides fluorescence functions to the GO fiber. Due to the 3D structure of the fiber, all FND on the fiber surface cannot be simultaneously excited in a single optical section image.

GO fibers were also decorated with SWCNH dahlias. Based on their physical and textural properties, such as high specific surface, high mechanical strength and high electrical and thermal conductivity, SWCNH have been studied for various potential applications [36,37]. SWCNH are highly hydrophobic and oxidation treatments are commonly needed to obtain stable aqueous SWCNH dispersions. However, we found out that tectomers assist SWCNH dispersibility in an aqueous SWCNH/tectomer mixture with only gentle agitation (Fig. 6(a)). The obtained dispersions remain stable for several months. A XPS study was performed to gain further insights into the nature of the interaction between tectomers and SWCNH. The N 1s XPS core level regions are compared in Fig. 6(b). As only the oligoglycine molecule contains nitrogen, changes in N 1s XPS spectra can be interpreted in terms of the established interactions by tectomers. The peak at 399.6 eV, corresponds to the nitrogen atoms in the oligoglycine antennae in tectomers. The shift towards higher BE in the presence of SWCNH (1.2 eV) suggests donation of electron density from amino groups in tectomers to the  $\pi$  system of SWCNH, in a similar manner to the electron donation from amines to CNT sidewalls described in the literature [38,39]. TEM images show that SWCNH were not embedded in tectomers but lying on the tectomer surface (Fig. 6(c, d)), in contrast to what we observed for MWCNT-COOH/tectomer hybrids, as the negatively charged carboxylic groups in MWCNT-COOH establish additional electrostatic interactions with positively charged protonated amino groups in tectomers, which favors tectomer platelet curvature resulting in adaptive coatings around MWCNT-COOH [20]. As a consequence, the large surface area and porosity of SWCNH should not be compromised in the resulting SWCNH/tectomer hybrids and coatings. Fig. 6(e, f) shows that GO fiber immersion

in these SWCNH/tectomer hybrid dispersions results in extensive thin SWCNH coatings that resisted through water washing procedures.

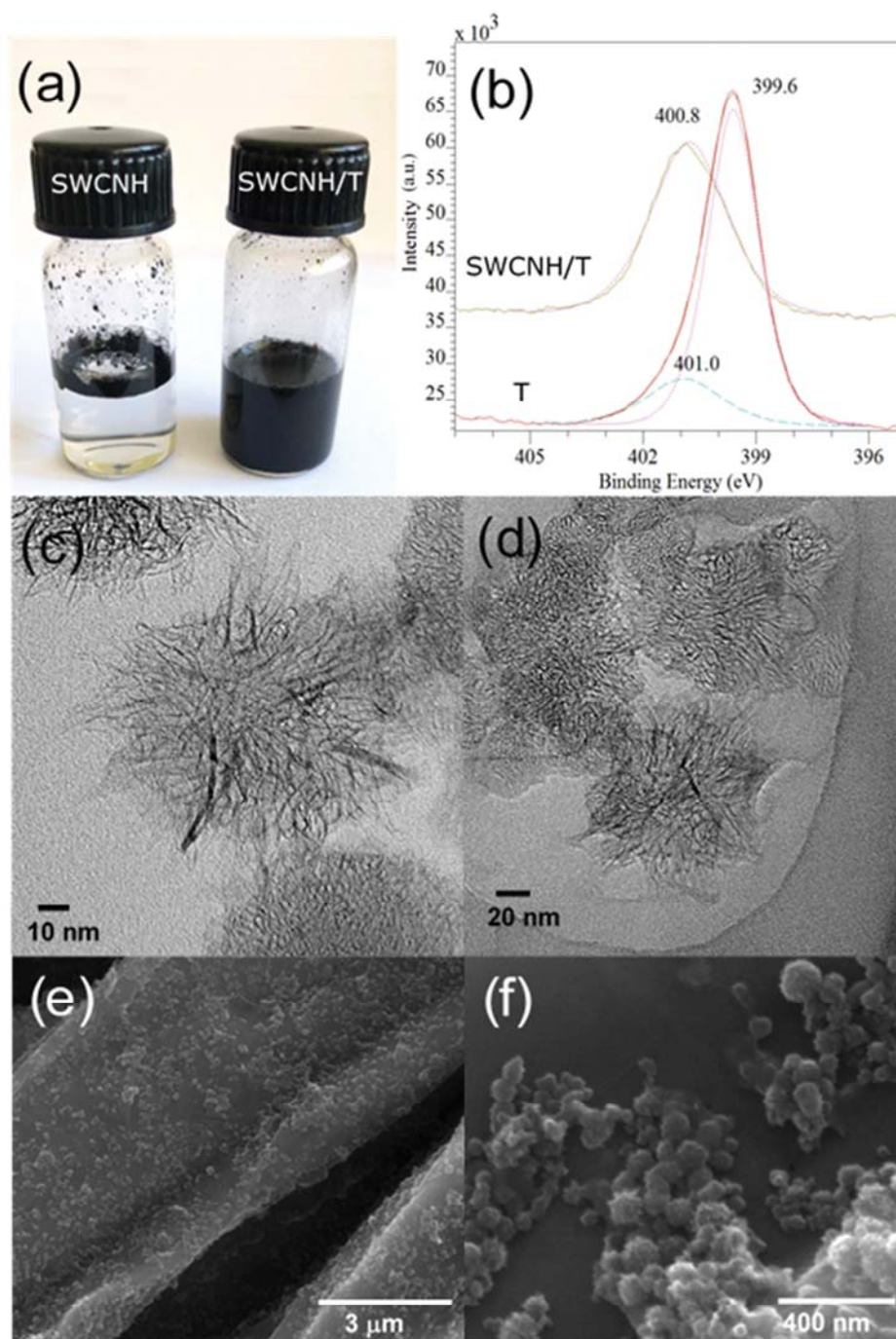


**Fig. 6.** Picture (a) shows that SWCNH are non-soluble in water, but tectomers (T) remarkably improve SWCNH dispersion in water by simply manually agitating a  $0.5 \text{ mg}\cdot\text{mL}^{-1}$  SWCNH/ $1 \text{ mg}\cdot\text{mL}^{-1}$  oligoglycine mixture in water. These dispersions are stable for several months. Comparison of high resolution N 1s XPS spectra of tectomers and SWCNH/tectomer hybrids (b). TEM characterization of SWCNH material (c), and of  $0.5 \text{ mg}\cdot\text{mL}^{-1}$  SWCNH/ $1 \text{ mg}\cdot\text{mL}^{-1}$  oligoglycine dispersion in water (d). SEM images of SWCNH/tectomer decorated GO fiber (e, f).

CNC materials comprise both cone- and disc-shaped particles. CNC consist of several nanometer thick layers of stacked graphene sheets, that in the case of cones can be considered 3D microparticles, whose height and radius are of the same order of magnitude [40]. We found that tectomers assist dispersion of highly hydrophobic CNC (Fig. 7(a)) by means of a similar interaction to that described above for SWCNH. Thus, N 1s XPS spectra (Fig. 7(b)) exhibit a shift (1.6 eV) towards higher EB, that can also be explained by charge transfer of amine groups to the  $\pi$  system of CNC. The larger shift in XPS spectra for CNC than for SWCNH suggests a stronger interaction in the case of CNC, as the interfacial interaction per unit area with tectomers will be maximized due to the more planar structure of CNC (Fig. 7(c, d)). However, in this case, the larger size of particles in CNC leads to complete precipitation of CNC/tectomer hybrids after ~24 hours. (Fig. S4). Extensive CNC coating of GO fibers was obtained after immersion of the fiber in a CNC/tectomer solution, followed by washing with water (Fig. 7(e, f)).

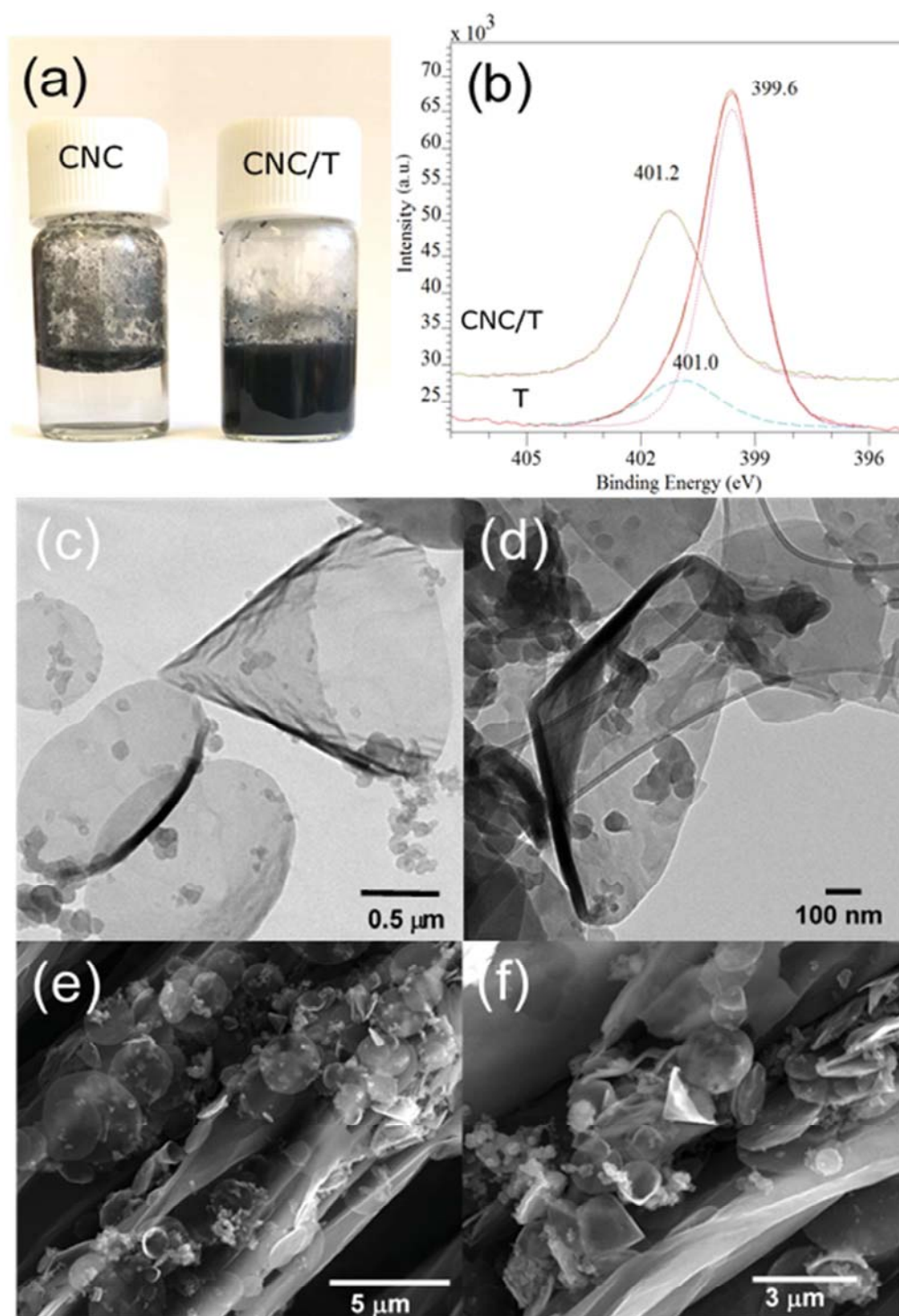


**Fig. 7.** Picture (s) shows that CNC are non-soluble in water, but tectomers (T) assist CNC dispersion in water by simply manually agitating a  $0.5 \text{ mg}\cdot\text{mL}^{-1}$  CNC/ $1 \text{ mg}\cdot\text{mL}^{-1}$  oligoglycine mixture in water. These dispersions are however not stable and fall out of solution over time (Fig. S4). Comparison of high resolution N 1s XPS spectra of tectomers and CNC/tectomer hybrids (b). TEM micrographs of CNC material (c), and  $0.5 \text{ mg}\cdot\text{mL}^{-1}$  CNC/ $1 \text{ mg}\cdot\text{mL}^{-1}$  oligoglycine dispersion in water (d). SEM images of CNC/tectomer decorated GO fiber (e, f).

### *3.2. Decoration of GO fibers with metal and polymer nanoparticles*

Metal NP coatings provide attractive functionalities for textiles and other substrates. As an example, AuNP coatings impart antibacterial, UV-blocking, colorfastness to washing and light irradiation, and increase thermal conductivity to common textiles [41-43]. On the other hand, PtNP immobilization on fiber surfaces and coatings has been exploited for catalyst, solar cell, and antibacterial applications [44-48]. Fiber impregnation with FeNP provides magnetic and antifungal functions to garments, and can be used in photocatalysis and for magnetic resonance (MR) imaging in biomedical applications [49-51].

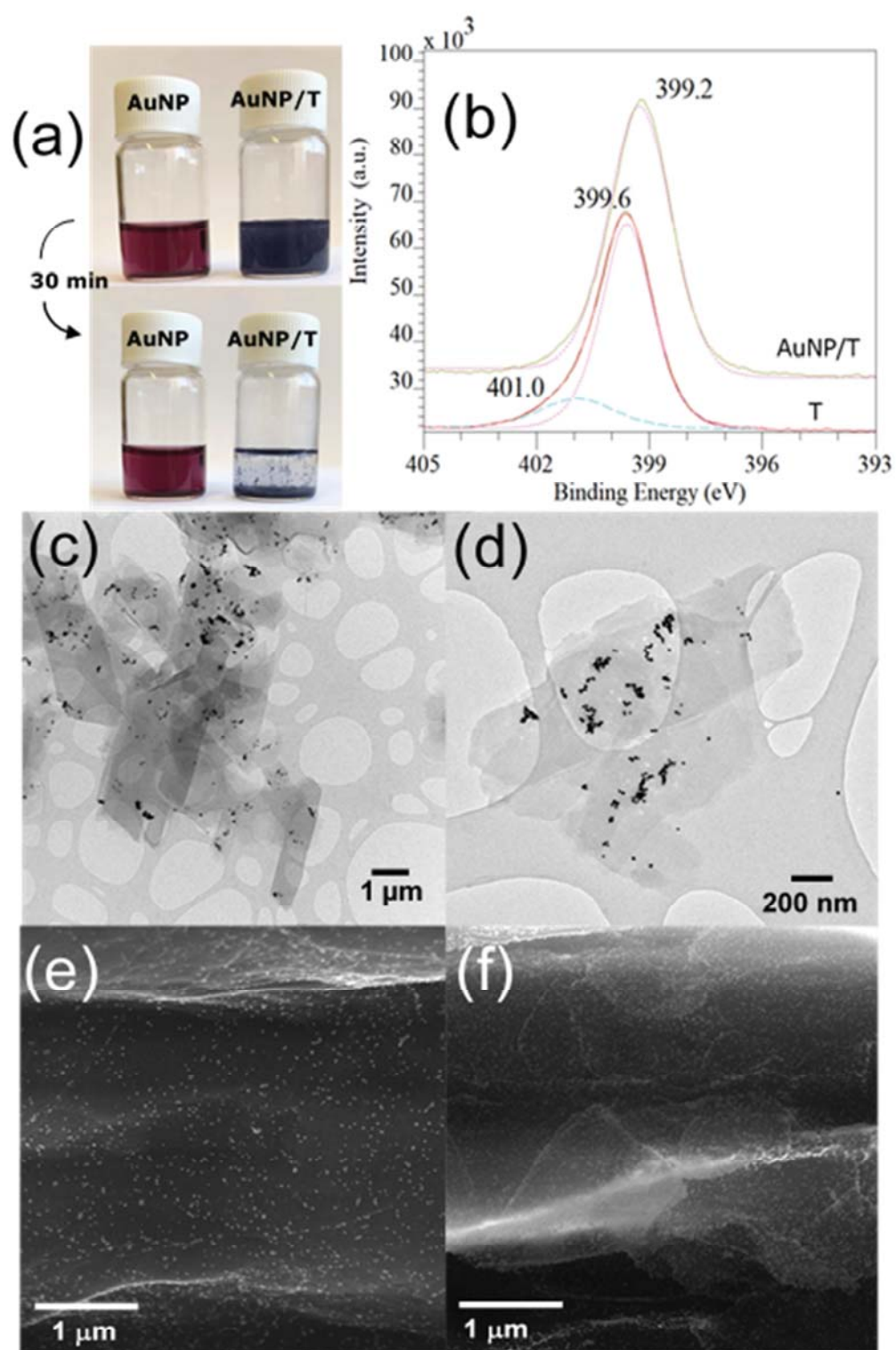


**Fig. 8.** Pictures showing  $0.05 \text{ mg}\cdot\text{mL}^{-1}$  AuNP (red) and  $0.05 \text{ mg}\cdot\text{mL}^{-1}$  AuNP/ $1 \text{ mg}\cdot\text{mL}^{-1}$  oligoglycine (blue) dispersions in water (AuNP/T), and evolution with time, leading to AuNP/tectomer precipitation due to neutralization of citrated AuNP charges by the protonated tectomer amino terminal groups in the AuNP/tectomer hybrid formation (a). Comparison of high resolution N 1s XPS spectra of tectomers and their corresponding hybrids with AuNP (b). TEM micrographs show AuNP/tectomer hybrids, where AuNP are only attached to tectomer platelets and not on the TEM grids (c, d), which highlights the strong AuNP/tectomer affinity. SEM images of AuNP- and AuNP/tectomer decorated GO fibers (e) and (f), respectively, showing that the adhesive properties of tectomers favors AuNP immobilization, leading to a higher AuNP density on the GO fiber surface, which is confirmed by EDS analysis (Fig. S5).

In order to evaluate the feasibility of metal NP decoration of GO fibers and fabrics using the adhesive properties of tectomers, we tested hydrophilic AuNP (Fig. 8), PtNP (Fig. 9) and FeNP (Fig. 10). While all tested NP exhibited strong tectomer interactions, particle size and the nature of the coatings dictated NP/tectomer hybrid stability in solution. AuNP bear a negative charge due to adsorbed citrate molecules on their surface and, therefore, effectively attach to tectomers by electrostatic interactions with protonated amino groups. Indeed, the addition of tectomer solution makes the red AuNP solutions turn blue (Fig. 8(a)) and aggregation occurs due to neutralization of the citrate charges around AuNP, resulting in Au/tectomer precipitate and a clear supernatant. These observations indicate the strong AuNP/tectomer interaction, which was

further confirmed by TEM (Fig. 8(c, d)). Hybridization of tectomers with PVP functionalized PtNP through hydrogen bond formation, however, led to the formation of stable PtNP/tectomer hybrid aqueous dispersions. Likewise, we observed that binding tectomers to FeNP further assisted FeNP dispersion, preventing FeNP aggregation and keeping FeNP in solution for several months. Here, interactions both with carboxy and hydroxy-groups on the carbon shell of FeNP come into play. High resolution N 1s XPS spectra of tectomer and AuNP/tectomer- or FeNP/tectomer hybrids are compared in Figs. 8(b) and 10(b), respectively. The peak at 399.6 eV corresponds to the nitrogen atoms in the oligoglycine antennae in tectomers. The 0.4 eV shift to lower BE, both in the AuNP/tectomer- and FeNP/tectomer hybrids spectra, suggests donation of electron density from oxygen groups in metal NP coatings to the amino groups in tectomers. A similar shift to lower BE (0.3 eV) was measured for GO/tectomer hybrids [20]. The N 1s XPS signal of tectomers is overlapped with that corresponding to the PVP coatings in PtNP, so the shift cannot be studied for PtNP/tectomer hybrids. On the other hand, the peak at 401.0 eV in tectomers, which can be assigned to the protonated amino groups ( $\text{NH}_3^+$ ), disappears in the metal NP/tectomer hybrids, which also can be explained by the donation of electron density from oxygen groups in metal NP coatings to tectomers. Moreover, according to high resolution Au 4f and Fe 2p XPS spectra (Fig. S6), shifts to higher BE in the metal NP/tectomer hybrids suggest that oxygen atoms in the metal NP coatings borrow electron density from the more electropositive metal atoms.

GO fibers were decorated with metal NP by immersion of tectomer-coated GO fibers in AuNP and PtNP dispersions (Figs. 8(f) and 9(d, f), respectively). However, FeNP GO fiber decoration was performed by direct immersion in FeNP/tectomer dispersion, rather than the two step method, due to the poor stability of FeNP dispersions in water (Fig. 10(a)). Tectomers

provided enhanced NP adhesion and water resistant properties, which was confirmed by EDS analysis (Figs. S5 and S7).

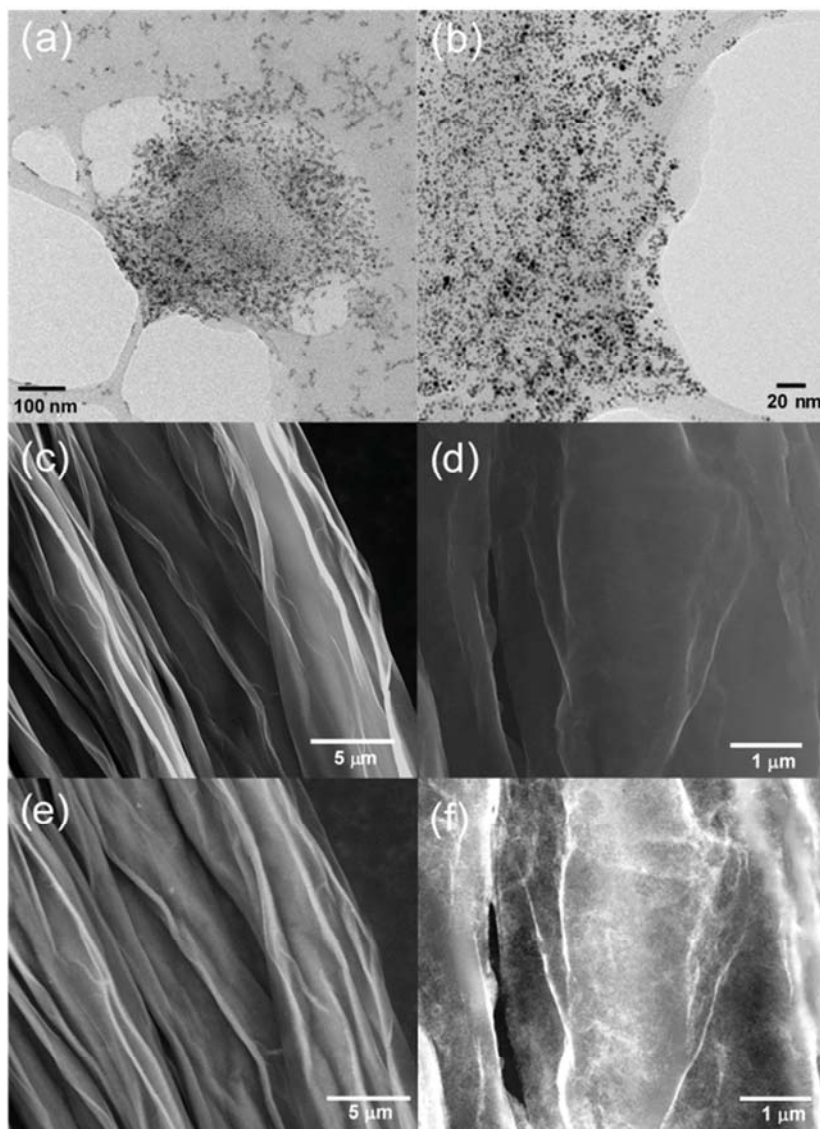


**Fig. 9.** TEM micrographs corresponding to  $4 \text{ mg}\cdot\text{mL}^{-1}$  PtNP/ $1 \text{ mg}\cdot\text{mL}^{-1}$  oligoglycine dispersions in water (a, b). SEM images of PtNP- and PtNP/tectomer decorated GO fibers, (c) and (d), respectively. BSE imaging of PtNP- and PtNP/tectomer decorated GO fibers, (e) and (f), respectively. These images show that PtNP immobilization on

GO fiber surface is significantly increased by means of tectomer adhesive properties, which was confirmed by EDS analysis (Fig. S7).

ACCEPTED MANUSCRIPT

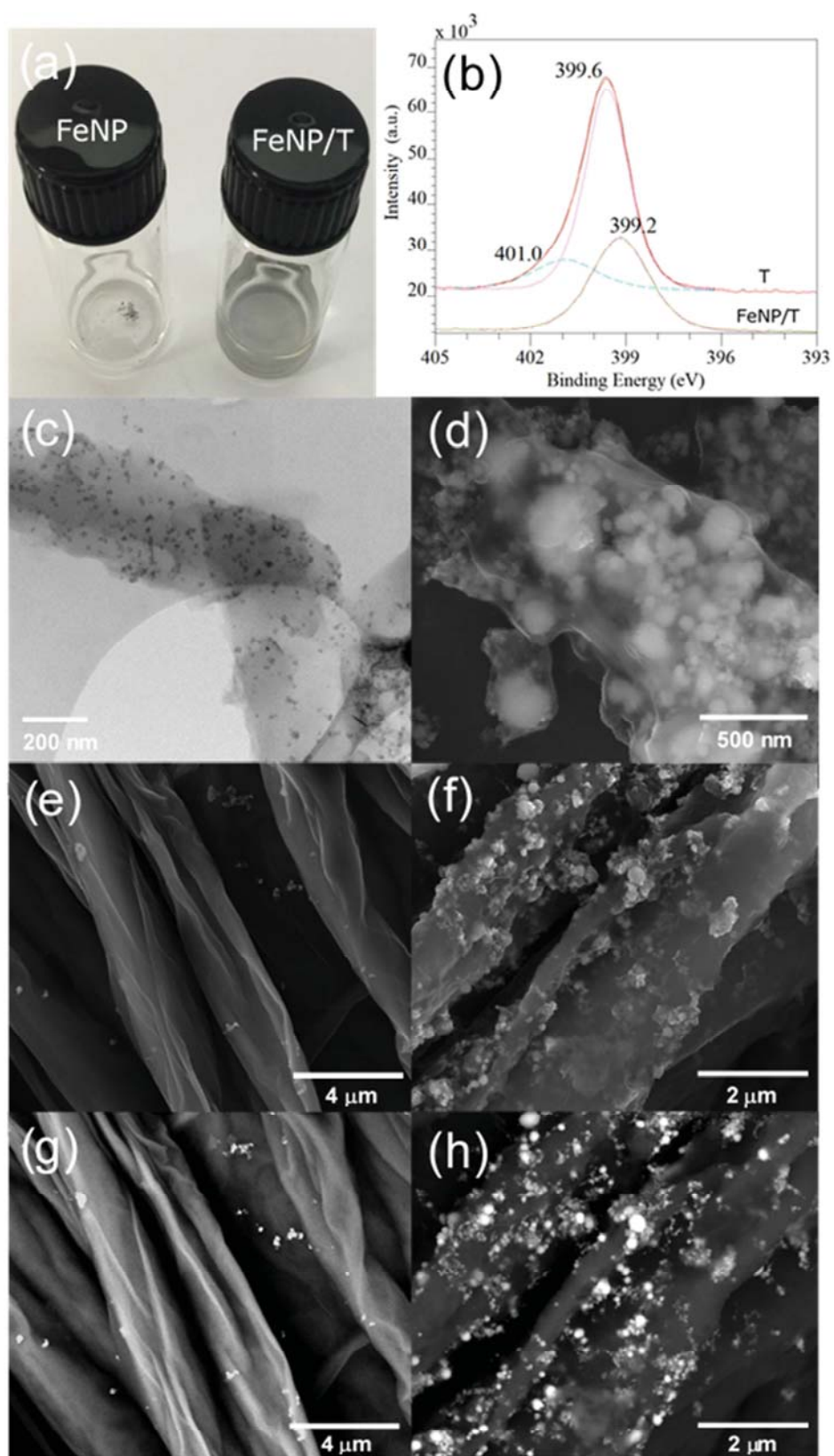


**Fig. 10.** Picture showing that tectomers (T) assist FeNP dispersion in aqueous solution, preventing nanoparticle aggregation and leading to stable FeNP/tectomer dispersions (a). Comparison of high resolution N 1s XPS spectra of tectomers and their corresponding hybrids with FeNP (b). TEM (c) and SEM (d) micrographs corresponding to  $0.2 \text{ mg}\cdot\text{mL}^{-1}$  FeNP/ $1 \text{ mg}\cdot\text{mL}^{-1}$  oligoglycine dispersions in water, showing FeNP attached on tectomer platelets. SEM images of FeNP- and FeNP/tectomer decorated GO fibers, (e) and (f), respectively; BSE imaging of FeNP- and FeNP/tectomer decorated GO fibers, (g) and (h), respectively. These images show that FeNP immobilization on GO fiber surface is significantly increased by means of tectomer adhesive properties.

Citrate-coated AuNP are commonly used for the synthesis of AuNP/nanocarbon hybrids [52]. For MWCNT-COOH, electrostatic repulsion between negative charges is detrimental for the formation of these hybrids, preventing the AuNP attachment to the MWCNT-COOH sidewalls (Fig. S8(a, c)). However, AuNP immobilization can be achieved by simply mixing AuNP dispersions with MWCNT-COOH/tectomer inks (Fig. S8(b, d)), due to the favorable interactions established between negatively-charged citrate groups in AuNP and the positively-charged protonated amino groups in the MWCNT-COOH/tectomer hybrids. Likewise, MWCNT-COOH/tectomer coated GO fibers were decorated with AuNP, as shown in (Fig. S8(e, f)). The hybrids shown here may be used for electrochemical biosensor applications similar to those already reported for AuNP/MWCNT-COOH/polydopamine hybrids [53]. On the other hand, this ability of tectomers to stick to both MWCNT-COOH and AuNP can be extended to

the synthesis of other metal NP/MWCNT-COOH hybrids, and might be of interest for catalysis applications [2].

Acrylate-based polymers form uniform and spherical (~160 nm in diameter) NP with a high concentration of COOH groups. Such NP have been used as nanocarriers for dental applications by complexing them with metal cations, such as  $\text{Ca}^{2+}$  and  $\text{Zn}^{2+}$  [54]. We expected that the oxygen functional groups on the polymer NP surface would enable strong interactions with tectomer amino terminal groups. We confirmed that tectomers conform and wrap around polymer NP (Fig. 11(a, b)). Moreover, we found that the amount of polymer NP decorating GO fibers was significantly increased using the adhesive properties of tectomers (Fig. 11(c, d)). Polymer NP are immobilized as thin, water resistant NP coatings.

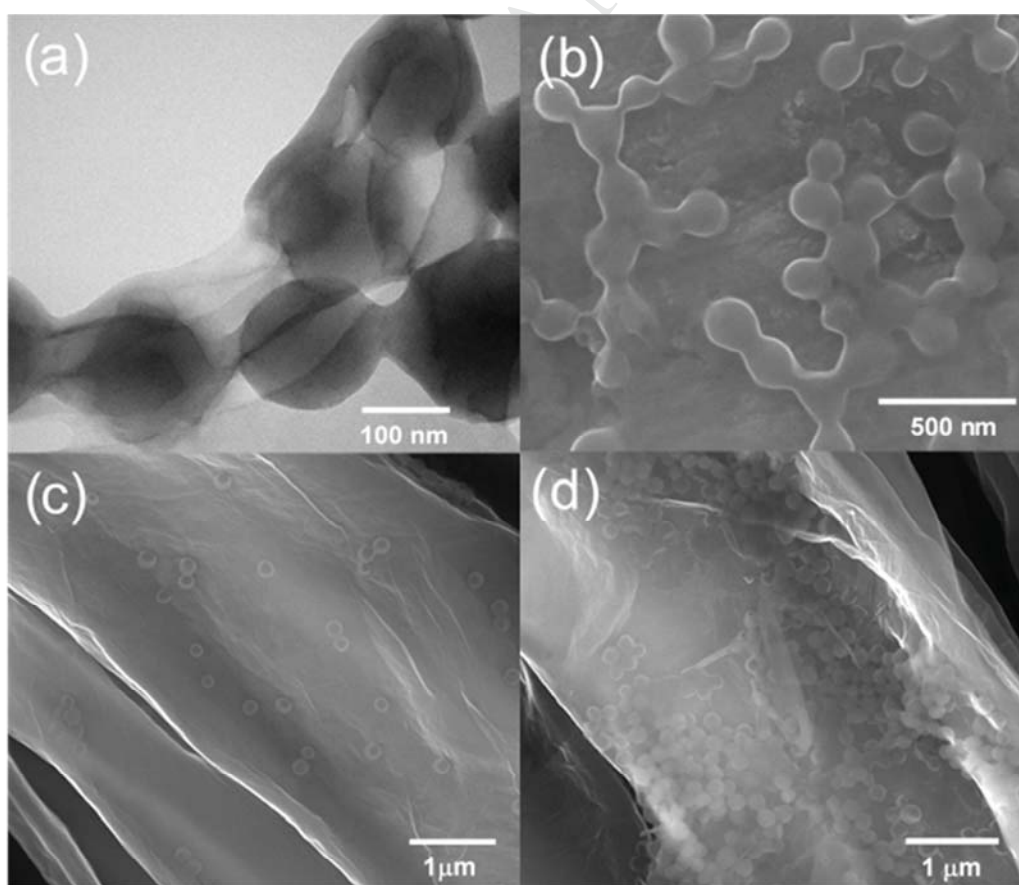


**Fig. 11.** TEM (a) and SEM (b) images corresponding to  $0.25 \text{ mg}\cdot\text{mL}^{-1}$  acrylated-based polymer NP/ $1 \text{ mg}\cdot\text{mL}^{-1}$  oligoglycine aqueous solution. SEM images of polymer NP- and polymer NP/tectomer decorated GO fibers, (c) and (d), respectively, showing that polymer nanoparticles immobilization on GO fiber surface is significantly increased by means of the adhesive properties of tectomers.

### *3.3. Decoration of GO fibers with drugs and fluorophores*

The efficient loading capability of tectomer nanocarriers of the fluorescent anticancer drug coralyne in solution was demonstrated by our group in a previous work [18]. The incorporation of drugs and active ingredients in fibers and fabrics has already made an impact in the marketplace, from the fabrication of wound dressings to smart textiles [55-59]. Now we tested if we could immobilize coralyne on the surface of GO fibers by immersion in an aqueous solution of coralyne-loaded tectomers. Confocal fluorescence microscopy shows that coralyne was more efficiently attached to GO fibers by means of the adhesive properties of tectomers and resisted water washing procedures (Fig. 12(a, b)). A number of interesting drug delivery and imaging applications could be envisaged for these coralyne-coated GO fibers and could be extended to other fluorescent drugs and dyes.

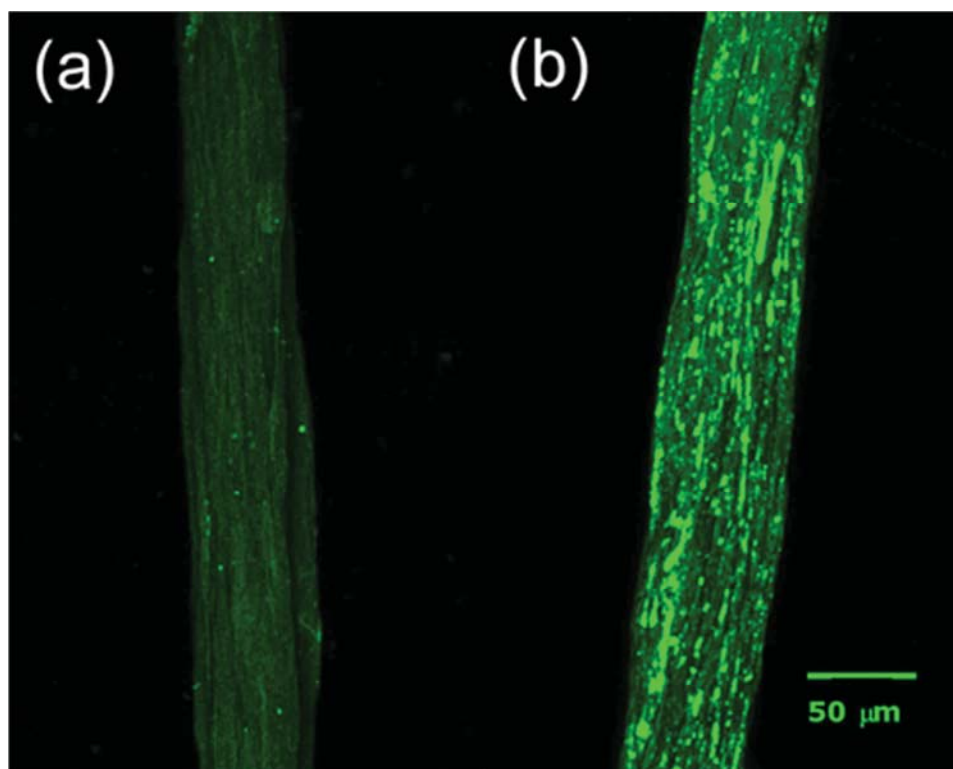


**Fig. 12.** Fluorescent drug coralyne immobilization on GO fibers. Comparison of fluorescence properties for GO fibers immersed in a  $15 \mu\text{g}\cdot\text{mL}^{-1}$  drug solution (a) and in a  $15 \mu\text{g}\cdot\text{mL}^{-1}$  drug/  $1 \text{mg}\cdot\text{mL}^{-1}$  oligoglycine solution (b), under the same experimental conditions. Confocal fluorescence images show higher coralyne concentration when fiber impregnation was performed with drug-loaded tectomers, which efficiently attach to GO fibers and resist water washing procedures.

#### *3.4. Nanomaterial decoration of other fibers*

The use of tectomer adhesives for surface functionalization can be extended to other fibers and substrates. We used this approach for the functionalization of PU/PEDOT:PSS (Figs. 13, 14 and S9), PMMA (Fig. S10), and PES fibers (Fig. 15). Strain-responsive PU/PEDOT:PSS

elastomeric composite fibers with high electrical conductivity offer great potential for applications in motion sensing, biomedical monitoring and stretchable electronics [60,61]. PU/PEDOT:PSS fibers at 13 wt. % (PEDOT:PSS),  $\sim 50 \mu\text{m}$  in diameter (Fig. 13(a, b)), exhibit electrical conductivity of up to  $\sim 10 \text{ S}\cdot\text{cm}^{-1}$ , and outstanding mechanical properties [28]. These fibers can be efficiently coated by tectomers (Fig. 13(c, d)).

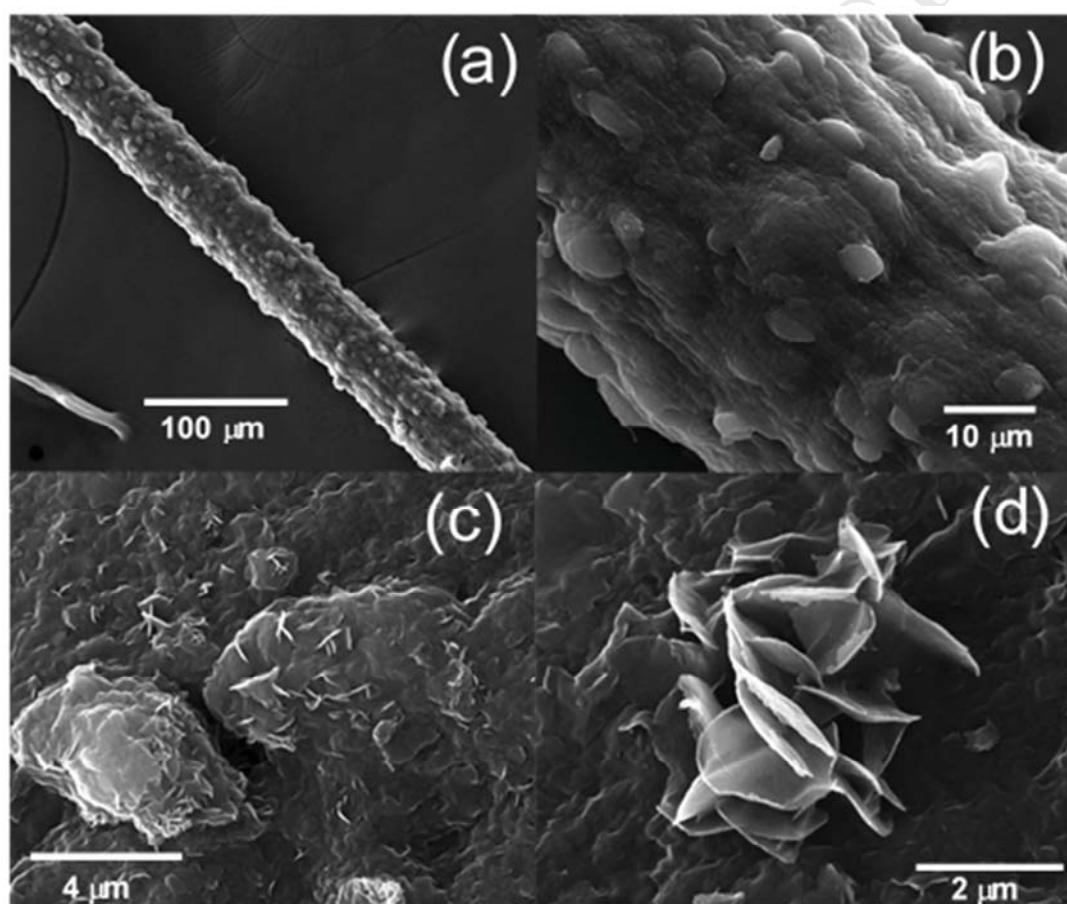


**Fig. 13.** SEM image of  $\sim 50 \mu\text{m}$  average diameter PU/PEDOT:PSS fiber (a, b). SEM images of tectomer coatings on these fibers (c, d).

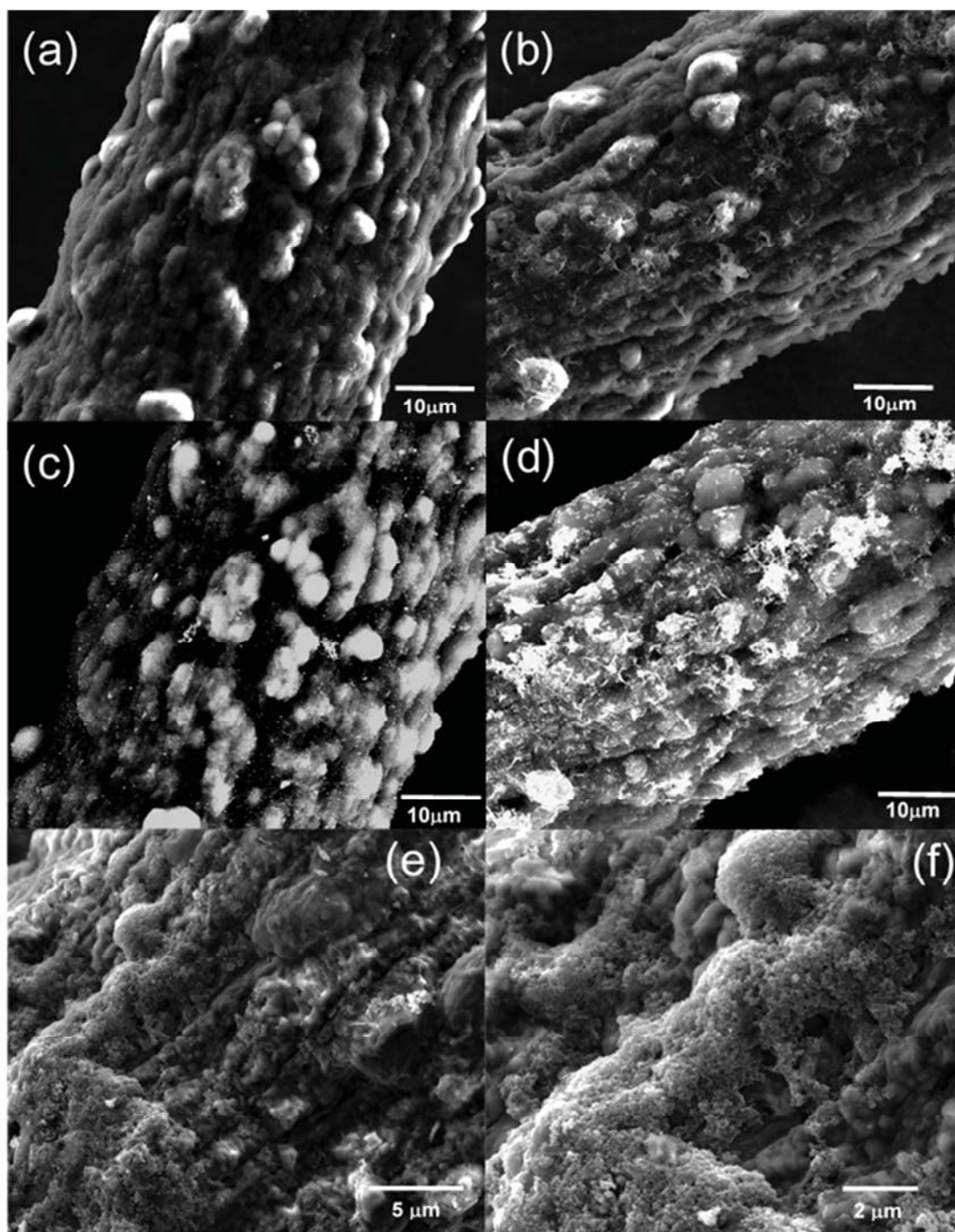


**Fig. 14.** SEM characterization of AuNP- and AuNP/tectomer decorated PU/PEDOT:PSS fiber (a) and (b), respectively; BSE imaging of AuNP- and AuNP/tectomer decorated PU/PEDOT:PSS fiber (c) and (d), respectively. These

images show that adhesive properties of tectomers favors AuNP immobilization leading to a higher AuNP concentration on the PU/PEDOT:PSS fiber surface, which was confirmed by EDS analysis (Fig. S9). SEM images of SWCNH/tectomer decorated PU/PEDOT:PSS fiber (e, f).

We also exploited the adhesive properties of tectomers to coat  $\sim 400$   $\mu\text{m}$  diameter PMMA (Fig. S10) and PES fibers (Fig. 15(b)). For all fiber samples tested we achieved successful tectomers-based fiber functionalization with SWCNH dahlia (Fig. S10(c, d) and (Fig. 14(e, f)), AuNP (Fig. 14(c, d) and Fig. S9 (b)), and MWCNT-COOH (Fig. 15(d)). It is worth noting that MWCNT-COOH poorly interacts with PES fabrics (Fig. 15(c)), due to electrostatic repulsions with abundant oxygen groups in PES. However, tectomer adhesive properties increase MWCNT-COOH immobilization (Fig. 15(d)). Electrical resistance measurements show that tectomer-mediated MWCNT-COOH coatings confer electrical conductivity to PES fabrics (electrical resistance values in the range of 10-90  $\text{M}\Omega$ , Fig. 15(f)), which makes it attractive for a variety of electronic textile applications. These results further highlight the enormous potential of tectomer coatings for the functionalization of different fiber materials, fiber architectures and fabrics.

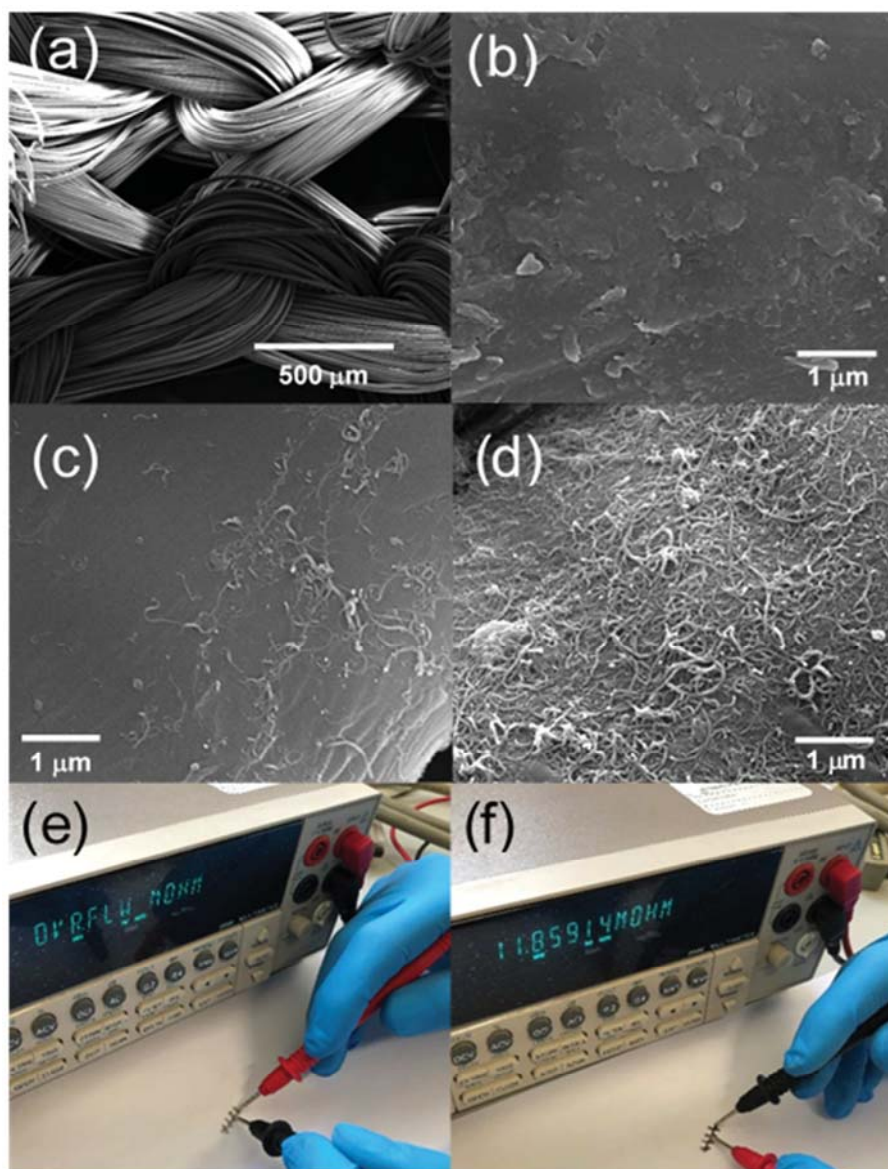


**Fig. 15.** SEM image of a PES fabric (a) and of tectomer coatings on this fabric (b), showing that tectomers resist water washing procedures. SEM images of a PES fiber after direct immersion in a 1 mg·mL<sup>-1</sup> MWCNT-COOH dispersion (c), and after a two-step procedure, first coated with tectomers by immersion in 1 mg·mL<sup>-1</sup> oligoglycine solution, followed by impregnation in a 1 mg·mL<sup>-1</sup> MWCNT-COOH

dispersion (d). Thus, the density of MWCNT-COOH on the fiber surface drastically increased when using tectomer adhesives. Two-probe electrical resistant measurements performed in PES fabrics of samples (e) and (f), showing that the water resistant tectomer-assisted MWCNT-COOH coatings in (d) provide electrical conductivity function to the fabric.

#### 4. Conclusions

The versatile surface chemistry of tectomers has been successfully used here for efficient GO and rGO fiber functionalization. Tectomers act as supramolecular adhesive for nanomaterial and molecule immobilization on the GO fiber surface. Tectomer-based coatings exhibit remarkable water resistant properties, and provide additional fiber structural protection during functionalization procedures. The tectomer-assisted functionalization strategy described here was extended to PU/PEDOT:PSS, PMMA and PES fibers and fabrics, and can potentially be used for many substrates. The physicochemical properties and applications of the resulting coatings can be tailored on demand by choosing the appropriate nanomaterial or molecule. Thus, MWCNT-COOH/tectomer coatings provide electrical conductivity to insulating fibers, whereas the tectomer-mediated attachment of fluorescent molecules and drugs can impart imaging and therapeutic functions. Interestingly, tectomers can enhance the water dispersive properties of highly hydrophobic carbon nanomaterials such as SWCNH and CNC, assisting their chemical processing. A wide range of applications can be envisaged for tectomer-mediated functionalized fibers, fabrics and substrates such as for energy storage, sensor, imaging, biomedical and antimicrobial applications, in catalysis, and for electronic- and smart textiles.

## Acknowledgement

Authors thank the Fundación Domingo Martínez (Ayudas a la Investigación 2013) and Diputación General de Aragón (Grupo de Nanosensores y Sistemas Bioanalíticos (N&SB), ref. E25\_17R) for research funding. MT would like to acknowledge University of Sussex strategic development fund. JMR acknowledges funding from the Australian Research Council (DP170102859). The TEM, and SEM microscopy work has been conducted in the "Laboratorio de Microscopías Avanzadas" at "Instituto de Nanociencia de Aragón - Universidad de Zaragoza". The authors acknowledge the LMA-INA for offering access to their instruments and expertise. The authors thank Alfonso Ibarra, Rodrigo Fernández-Pacheco, Carlos Cuestas, Gala Simón, Isabel Rivas and Isaías Fernández for valuable technical support and fruitful discussions. Polymer NP samples were kindly supplied by NanoMyP<sup>®</sup>, Nanomateriales y Polímeros S.L., [www.nanomyp.com](http://www.nanomyp.com).

## Appendix A. Supplementary data

Supplementary data to this article can be found online at <https://>

## References

- [1] J.H. Ryu, P.B. Messersmith, H. Lee, Polydopamine surface chemistry: a decade of discovery, *ACS Appl. Mater. Interfaces* 10 (2018) 7523-7540.
- [2] M.E. Lyngé, R. van der Westen, A. Postma, B. Städler, Polydopamine - a nature inspired polymer coating for biomedical science, *Nanoscale* 3 (2011) 4916-4928.

- [3] S.T. Koev, P.H. Dykstra, X. Luo, G.W. Rubloff, W.E. Bentley, G.F. Payme, et al. Chitosan: an integrative biomedical for a lab-on-a-chip, *Lab Chip* 10 (2010) 3026-3042.
- [4] N. Mati-Baouche, P.-H. Elchinger, H. de Baynast, G. Pierre, C. Delattre, P. Michaud, Chitosan as adhesive, *Eur. Pol. J* 60 (2014) 198-212.
- [5] A. Baranwal, A. Kumar, A. Priyadharshini, G.S. Oggu, I. Bhatnagar, A. Srivastava, P. Chandra, The chemistry of tissue adhesive materials, *Int. J. Biological Macromolecules* 110 (2018) 110-113.
- [6] S.E. D'Souza, M.H. Ginsberg, E.F. Plow, Arginyl-glycyl-aspartic acid (RGD): a cell adhesion motif, *Trends Biochem. Sci.* 16 (1991) 246-250.
- [7] B.T. Houseman, M. Mrksigh, The microenvironment of immobilized Arg-Gly-Asp peptides is an important determinant of cell adhesion, *Biomaterials* 22 (2001) 943-955.
- [8] P.J.M. Bouten, M. Zonjee, J. Bender, S.T.K. Yauw, H. van Goor, J.C.M. van Hest, et al., The chemistry of tissue adhesive materials, *Progress Pol. Sci.* 39 (2014) 1375-1405.
- [9] M.W. Grinstaff, Designing hydrogel adhesives for corneal wound repair, *Biomaterials* 28 (2007) 5205-5214.
- [10] Y.K. Jo, H.J. Kim, Y. Jeong, K.I. Joo, H.J. Cha, Biomimetic surface engineering of biomaterials by using recombinant mussel adhesive proteins, *Adv. Mater. Interfaces* 5 (2018) 1800068.
- [11] S.V. Tsygankova, A.A. Chinarev, A.B. Tuzikov, N. Severin, A.A. Kalachev, J.P. Rabe, et al., Biantennary oligoglycines and glyco-oligoglycines self-associating in aqueous medium, *Beilstein J. Org. Chem.* 10 (2014) 1372-1382.

- [12] S.V. Tsygankova, A.A. Chinarev, A.B. Tuzikov, I.S. Zaitsev, N. Severin, A.A. Kalachev, et al., Assembly of oligoglycine layers on mica surface, *J. Biomater. Nanobiotechnol.* 2 (2011) 91-97.
- [13] N.V. Bovin, A.B. Tuzikov, A.A. Chinarev, Oligoglycines: materials with unlimited potential for nanotechnologies, *Nanotechnol. Russ.* 3 (2008) 291-302.
- [14] A.Y. Gyurova, S.V. Stoyanov, E. Mileva, Interaction of four-antennary oligoglycines and lipopolysaccharides in aqueous media, *Colloids Surf. A*, 460 (2014) 130-136.
- [15] A.B. Tuzikov, A.A. Chinarev, A.S. Gambaryan, V.A. Oleinikov, D.V. Klinov, N.B. Matsko, et al., Polyglycine II nanosheets: supramolecular antivirals?, *ChemBioChem* 4 (2003) 147-154.
- [16] N.V. Bovin, A.B. Tuzikov, A.A. Chinarev, A.S. Gambaryan, Multimeric glycotherapeutics: new paradigm, *Glycoconjugate J.*, 21 (2004) 471-478.
- [17] A. Almasian, N.M. Mahmoodi, M.E. Olya, Tectomer grafted nanofiber: synthesis, characterization and dye removal ability from multicomponent system, *J. Ind. Eng. Chem.* 32 (2015) 85-98.
- [18] R. Garriga, I. Jurewicz, E. Romero, C. Jarne, V.L. Cebolla, A.B. Dalton, et al., 2-Dimensional, pH-responsive oligoglycine-based nanocarriers, *ACS Appl. Mater. Interfaces* 8 (2016) 1913-1921.
- [19] I. Jurewicz, R. Garriga, M.J. Large, J. Burn, N. Bardi, A.A.K. King, et al., Functionalization of silver nanowire transparent electrodes with self-assembled 2-dimensional tectomer nanosheets, *ACS Appl. Nano Mater.* 1 (2018) 3903-3912.

- [20] R. Garriga, I. Jurewicz, S. Seyedin, N. Bardi, S. Totti, B. Matta-Domjan, et al., Biocompatible and pH-responsive carbon nanotube- and graphene oxide/tectomer hybrid composites and coatings, *Nanoscale* 9 (2017) 7791-7804.
- [21] X. Li, P. Sun, M. Zhu, K. Wang, M. Zhong, J. Wei, et al., Multifunctional graphene woven fabrics, *Sci. Rep.* 2 (2012) 395.
- [22] R. Jalili, S.H. Aboutaleb, D. Esrafilzadeh, R.L. Shepherd, J. Chen, S. Aminorroaya-Yamini, et al., Scalable one-step wet-spinning of graphene fibers and yarns from liquid crystalline dispersions of graphene oxide: towards multifunctional textiles, *Adv. Funct. Mater.* 23 (2013) 5345-5354.
- [23] R. Cruz-Silva, A. Morelos-Gomez, H. Kim, H. Jang, F. Tristan, S. Vega-Diaz, et al., Super-stretchable graphene oxide macroscopic fibers with outstanding knotability fabricated by dry film scrolling, *ACS Nano* 8 (2014) 5959-5967.
- [24] S. Seyedin, M.S. Romano, A.I. Minett, J.M. Razal, Towards the knittability of graphene oxide fibres, *Sci. Rep.* 5 (2015) 14946.
- [25] R. Cruz-Silva, M. Endo, M. Terrones, Graphene oxide films, fibers, and membranes, *Nanotechnol. Rev.* 5 (2016) 377-391.
- [26] J. Zhang, S. Seyedin, Z. Gu, N. Salim, X. Wang, J.M. Razal, Liquid crystals of graphene oxide: a route towards solution-based processing and applications, *Part. Part. Syst. Character.* 34 (2017) 1600396.

- [27] S.H. Aboutalebi, R. Jalili, D. Esrafilzadeh, M. Salari, Z. Gholamvand, S.A. Yamini, et al., High-performance multifunctional graphene yarns: toward wearable all-carbon energy storage textiles, *ACS Nano* 8 (2014) 2456-2466.
- [28] M.Z. Seyedin, J.M. Razal, P.C. Innis, G.G. Wallace, Strain-responsive polyurethane/PEDOT:PSS elastomeric composite fibers with high electrical conductivity, *Adv. Funct. Mater.* 24 (2014) 2957-2966.
- [29] A. Krisnan, E. Dujardin, M.M.J. Treacy, J. Hugdahl, S. Lynum, T.W. Ebbesen, Graphitic cones and the nucleation of curved carbon surfaces, *Nature* 388 (1997) 451-454.
- [30] C. Pagura, S. Barison, S. Battiston, M. Schiavon. Synthesis and characterization of single wall carbon nanohorns produced by direct vaporization of graphite, Conference Paper, Conference: Nanotechnology 2010: Advanced Materials, CNTs, Particles, Films and Composites - Technical Proceedings of the 2010 NSTI Nanotechnology Conference and Expo, NSTI-Nanotech 2010, vol. 1, 2010.
- [31] S. Kumar, K.S. Gandhi, R. Kumar, Modeling of formation of gold nanoparticles by citrate method, *Ind. Eng. Chem. Res.* 46 (2007) 3128-3136.
- [32] R.L. Harniman, O.J.L. Fox, W. Janssen, S. Drijkoningen, K. Haenen, P.W. May, Direct observation of electron emission from grain boundaries in CVD diamond by PeakForce-controlled tunnelling atomic force microscopy, *Carbon* 94 (2015) 386-395.
- [33] R. Marcilla, E. Muñoz, et al., in preparation.

- [34] X. Dong, G. Xing, M.B. Chan-Park, W. Shi, N. Xiao, J. Wang, et al., The formation of a carbon nanotube–graphene oxide core–shell structure and its possible applications, *Carbon* 49 (2011) 5071-5078.
- [35] M.H. Alkahtani, F. Alghannam, L. Jiang, A. Almethen, A. A. Rampersaud, R. Brick, C.L. Gomes, M.O. Scully, P.R. Hemmer, Fluorescent nanodiamonds: past, present, and future, *Nanophotonics* 7 (2018) 1423–1453.
- [36] Z. Shuyun, X. Guobao, Single-walled carbon nanohorns and their applications, *Nanoscale* 2 (2010) 2538-2549.
- [37] N. Karousis, I. Suarez-Martinez, C.P. Ewels, N. Tagmatarchis. Structure, properties, functionalization, and applications of carbon nanohorns, *Chem. Rev.* 116 (2016) 4850-4883.
- [38] M. Shim, A. Javey, N.W.S. Kam, H. Dai, Polymer functionalization for air-stable n-type carbon nanotube field-effect transistors, *J. Am. Chem. Soc.* 123 (2001) 11512-11513.
- [39] A. Star, J.-C.P. Gabriel, K. Bradley, G. Grüner, Electronic detection of specific protein binding using nanotube FET devices, *Nano Lett.* 3 (2003) 459-463.
- [40] E. Krisnan, M.M.J. Dujardin, J. Treacy, J. Hugdahl, S. Lynum, T.W. Ebbesen, Graphitic cones and the nucleation of curved carbon surfaces, *Nature* 388 (1997) 451–454.
- [41] B. Tang, L. Sun, Y. Yu, X. Wang, In-situ synthesis of gold nanoparticles for multifunctionalization of silk fabrics, *Dyes Pigments* 103 (2014) 183-190.
- [42] S. Sharaf, A. Higazy, A. Hebeish, Utilization of gold nanoparticles in production of antibacterial cotton fabric, *Int. J. Curr. Res.* 7 (2015) 19264-19273.

- [43] B. Tang, X. Lin, Y. Fan, D. Li, J. Zhou, W. Chen, et al., In situ synthesis of gold nanoparticles on cotton fabric for multifunctional applications, *Cellulose* 24 (2017) 4547-4560.
- [44] S. Shahidi, M. Ghoranneviss, Investigation on dye ability and antibacterial activity of nanolayer platinum coated polyester fabric using DC magnetron sputtering, *Prog. Org. Coatings*. 70 (2011) 300-303.
- [45] A. Bragaru, E. Vasile, C. Obrega, M. Kusko, M. Danila, A. Radoi, Pt-nanoparticles on graphene – polyelectrolyte nanocomposite: investigation of H<sub>2</sub>O<sub>2</sub> and methanol electrocatalysis, *Mater. Chem. Phys.* 146 (2014) 538-544.
- [46] Z. Kang, X. Tan, X. Li, T. Xiao, L. Zhang, J. Lao, et al., Self-deposition of Pt nanoparticles on graphene woven fabrics for enhanced hybrid Schottky junctions and photoelectrochemical solar cells, *Phys.Chem.Chem.Phys.* 18 (2016) 1992-1997.
- [47] X. Li, L. Zhang, X. Zang, X. Li, H. Zhu, Photo-promoted platinum nanoparticles decorated MoS<sub>2</sub>@graphene woven fabric catalyst for efficient hydrogen generation, *ACS Appl. Mater. Interfaces* 8 (2016) 10866-10873.
- [48] W.-T. Chiu, C.-Y. Chen, T.-F. M. Chang, Y. Tahara, T. Hashimoto, H. Kurosu, et al., Platinum coating on silk by a supercritical CO<sub>2</sub> promoted metallization technique for applications of wearable devices, *Surf. Coat. Tech.* 350 (2018) 1028-1035.
- [49] S. Xu, D. Shen, P. Wu, Fabrication of water-repellent cellulose fiber coated with magnetic nanoparticles under supercritical carbon dioxide, *J. Nanopart. Res.* 15 (2013) 1577.

- [50] A. Nazari, M.R. Shishehbor, S.M. Poorhashemi, Enhanced magnetic and antifungal characteristics on wool Fe<sub>3</sub>O<sub>4</sub> nanoparticles and BTCA: a facile synthesis and RSM optimization, *J. Textile Ins.* 107 (2016) 1617-1631.
- [51] M.E. Mertens, S. Koch, P. Schuster, J. Wehner, Z. Wu, F. Gremse, et al., USPIO-labeled textile materials for non-invasive MR imaging of tissue-engineered vascular grafts, *Biomaterials* 39 (2015) 155-163.
- [52] A. Seral-Ascaso, A. Luquin, M.J. Lázaro, G.F. de la Fuente, M. Laguna, E. Muñoz, Synthesis and application of gold-carbon hybrids as catalysts for the hydroamination of alkynes, *Appl. Catal. A* 456 (2013) 88-95.
- [53] X. Dong, X. Lu, K. Zhang, Y. Zhang, Chronocoulometric DNA biosensor based on a glassy carbon electrode modified with gold nanoparticles, poly(dopamine) and carbon nanotubes, *Microchim. Acta.* 180 (2013) 101-108.
- [54] R. Osorio, E. Osorio, A.L. Medina-Castillo, M. Toledano, Polymer nanocarriers for dentin adhesion, *J. Dent. Res.* 93 (2014) 1258-1263.
- [55] J. Zeng, X. Xu, X. Chen, Q. Liang, X. Bian, L. Yang, et al., Biodegradable electrospun fibers for drug delivery, *J. Controlled Release* 92 (2003) 227-231.
- [56] J.S. Boateng, K.H. Matthews, H.N.E. Stevens, G.M. Eccleston, Wound healing dressings and drug delivery systems, *J. Pharmaceutical Sci.* 97 (2008) 2892-2923.
- [57] E. Pérez, L. Martín, C. Rubio, J.S. Urieta, E. Piera, M.A. Caballero, et al., Encapsulation of  $\alpha$ -tocopheryl acetate into zeolite Y for textile application, *Ind. Eng. Chem. Res.* 49 (2010) 8495-8500.

- [58] D. Esrafilzadeh, J.M. Razal, S.E. Moulton, E.M. Stewart, G.G. Wallace, Multifunctional conducting fibres with electrically controlled release of ciprofloxacin, *J. Controlled Release* 169 (2013) 313-320.
- [59] S. Hashemikia, N. Hemmatinejad, E. Ahmadi, M. Montazer, A novel cotton fabric with anti-bacterial and drug delivery properties using SBA-15-NH<sub>2</sub>/polysiloxane hybrid containing tetracycline, *Mater. Sci. Eng. C* 59 (2016) 429-437.
- [60] S. Seyedin, J.M. Razal, P.C. Innis, A. Jeiranikhameneh, S. Beirne, G.G. Wallace, Knitted strain sensor textiles of highly conductive all-polymeric fibers, *ACS Appl. Mater. Interfaces* 7 (2015) 21150-21158.
- [61] S. Seyedin, S. Moradi, C. Singh, J.M. Razal, Continuous production of stretchable conductive multifilaments in kilometer scale enables facile knitting of wearable strain sensing textiles, *Appl. Mater. Today* 11 (2018) 255-263.